Effect of noise on extreme events probability in a one-dimensional nonlinear Schrödinger equation

T.I. Lakoba*

Department of Mathematics and Statistics, 16 Colchester Ave.,
University of Vermont, Burlington, VT 05401, USA

February 1, 2015

Abstract

We report a numerical observation that multiplicative random forcing (noise) significantly increases the probability of formation of extreme events in the one-dimensional, focusing nonlinear Schrödinger equation. Furthermore, this phenomenon is sensitive to the noise's spatial correlation length. Highly correlated multiplicative noise may increase the probability of extreme events even when the average nonlinearity of the system is weak. On the contrary, noise with short spatial correlations substantially increases the probability of extreme events only for sufficiently strong average nonlinearity.

Keywords: Nonlinear Schrödinger equation, Extreme events, Rogue waves, Random forcing, Multiplicative noise.

*tlakoba@uvm.edu, 1 (802) 656-2610

1 Introduction

Occurrence of waves whose amplitude exceeds the average by several standard deviations has been actively studied in such diverse areas as nonlinear optics and water waves; see, e.g., recent reviews [1]–[4] and references therein. Below we will refer to such waves as rogue waves irrespective of the physical context in which they occur. The nonlinear Schrödinger equation (NLS) has been considered as a toy model that is capable of producing rogue waves, even though it significantly oversimplifies the underlying physics both in optics (see, e.g., [5]) and in the oceanic wave theory (see, e.g., [6]-[10] and references therein). Notably, the NLS model does predict a higher probability of observing rogue waves than the linear model.

In this letter we report a numerical observation that noise terms included in the NLS further increase the probability of rogue waves formation. Furthermore, certain types of noise do so considerably more than others, with a spatially highly correlated multiplicative noise resulting in the most prominent such an increase. We emphasize that since the NLS is only a toy model of rogue waves, then our stochastic modification of that equation is also meant only to exhibit a *trend* whereby a certain combination of nonlinearity, dispersion, and stochastic forcing results in a significant increase of the probability of rogue waves.

It should be noted that the stochastic NLS has also been extensively studied in diverse applications. For example, in fiber optical communications, additive noise has most often been used to model the effect of spontaneous emission from amplifiers, as the signal propagates in a transmission line (see, e.g., [11]), while multiplicative noise could model the effect of a fluctuating pump in a Raman amplifier (see, e.g., [12]). Most of those studies focused on how the noise affects a single soliton, although (wavelength-dependent) noise and damping were also considered in studies of wave turbulence (see, e.g., [13, 14] and references therein).

The model that we consider here is

$$iu_t + \beta u_{xx} + \gamma|u|^2 u = -i\alpha u - i\varepsilon u_{xxxx} + \xi + \eta u, \tag{1}$$

where β, γ are the dispersion and nonlinearity coefficients, α is a wavelength-independent damping coefficient, and the term εu_{xxxx} accounts for the energy loss at very high wavenumbers[1]. In the context of water waves, such a term can mimic, e.g., the effect of wavebreaking. Its inclusion in the model does not qualitatively affect its predictions but does allow us to avoid using a very wide spectral domain and hence a very small time step in our numerical simulations. The additive and multiplicative noises, ξ and η, are assumed to be complex-valued, independent of each other, and having zero average and the following correlation functions:

$$\langle \xi^*(x_1,t_1)\xi(x_2,t_2)\rangle = 2D(|x_1-x_2|)\delta(t_1-t_2), \tag{2a}$$

$$\langle \eta^*(x_1,t_1)\eta(x_2,t_2)\rangle = 2C(|x_1-x_2|)\delta(t_1-t_2), \tag{2b}$$

$$\langle \xi(x_1,t_1)\xi(x_2,t_2)\rangle = \langle \eta(x_1,t_1)\eta(x_2,t_2)\rangle = 0, \tag{2c}$$

[1] In [13, 14], damping terms that accounted for even higher x-derivative of u, were considered.

where $\langle \ldots \rangle$ denotes averaging over an ensemble of noise realizations, the asterisk denotes a complex conjugate, and D and C are real-valued. In time, the noises are treated in the Stratonovich sense (see, e.g., Chap. 5 in [15]), whereby their correlation time is assumed to be much smaller than any other time scale in the model, but still finite.

In space, the noises must have finite (essentially nonzero) correlation lengths because, as we will show below, the spatial scale of the solution u is of the same order. A spatially correlated noise can be related to a spatially uncorrelated noise w, whose Fourier transform satisfies $\langle \hat{w}^*(k_1,t_1)\hat{w}(k_2,t_2)\rangle = 2\delta(k_1-k_2)\delta(t_1-t_2)$ and $\langle \hat{w}(k_1,t_1)\hat{w}(k_2,t_2)\rangle = 0$, via

$$\{\xi(x,t),\, \eta(x,t)\} = \int G_{\{\xi,\eta\}}(k)\hat{w}_{\{\xi,\ \eta\}}(k,t)e^{-ikx}dk; \tag{3a}$$

here $\{\ldots\}$ denotes grouping of terms. Then

$$\{D(x),\, C(x)\} = \int |G_{\{\xi,\eta\}}(k)|^2 e^{-ikx}dk, \tag{3b}$$

and the fact that D and C are real implies that $|G_{\{\xi,\eta\}}(k)|^2$ are symmetric. In what follows we will use notations

$$D(0) \equiv D_0, \qquad C(0) \equiv C_0. \tag{3c}$$

In (3a) and everywhere below, if the limits of integration are not indicated, they are assumed to be infinite.

Let us note that within the framework of the NLS as a model for oceanic waves, a combination of the multiplicative noise and damping terms, $(-\alpha+\eta)u$, can be interpreted as a result of combined action of the wavelength-independent damping and the forcing due to wind [16, 17, 18]. Here $(-\alpha)$ is the net damping rate due to both wavelength-independent loss mechanisms and the constant part of wind forcing, while η is attributed to the variable part of the forcing. In the oceanic waves context, the interpretation of the additive noise, ξ, is less clear. However, we include it due to both a formal reason explained in the next paragraph as well as for the generality of our toy model. It will follow from our results that it is the multiplicative noise term that is responsible for the main effect reported in this work.

One of our key assumptions is that we consider the evolution and, in particular, formation of rogue waves in the *statistically steady* state of model (1). (Below we will omit the modifier 'statistically' for brevity.) This implies that there must be a balance, on average, between the influx of energy to the system due to noise and the energy dissipation due to the α- and ε-terms. In linear systems, such a balance is well known as a form of the fluctuation-dissipation theorem, whereby the intensity of noise and the dissipation rate in a steady state must be related (see Eq. (6) below). Note that this balance for a nonzero solution u in (1) can only be achieved for a nonzero additive noise: if a multiplicative noise alone is present, then the solution will either blow up (due to a purely linear mechanism) or decay to zero. Thus, if one neglects the ε-term for a moment, the constants α, D_0, and C_0 must be related by (6) to guarantee the existence of a steady state. It may seem, and perhaps is, unphysical that the damping rate α, which is an intrinsic property of the wave model, and the noise intensities D_0 and C_0, which characterize the noises external to the

model, are related. A more physical damping mechanism, at least for oceanic waves, may be one where energy is dissipated primarily in high wave numbers [13, 14]. The reason why we consider the situation where almost all energy is lost due to the wavelength-independent damping is that in this case, it is possible to control the time-average nonlinearity using some analytical estimates. Such a control is required for a careful determination of sources that affect our main conclusion.

Let us note that since it is the noise that drives the model into the steady state, then the spatial spectral bandwidth of the steady-state solution must, on average, be on the order of (or greater than) that of the noise. This simply follows from the fact that terms in (1) must balance out. If the noise contribution to (1) is considerably less than that of the nonlinear term, then the spectrum of noise can be narrower than the spectrum of the average solution. However, it cannot be wider (in the order of magnitude sense); indeed, a wide-band noise would excite high wavenumbers in the steady-state solution, thereby widening its spectrum. In our simulations, we have observed the spectral bandwidths of the solution and the noise to be within a factor of two from one another, except for the moments where a rogue wave would form, at which point the solution's bandwidth would considerably exceed that of the noise. This is the physical reason why we consider only correlated noises, as per (2), in this work. This situation should be contrasted to that in optical communications: The noise bandwidth there considerably exceeds that of the useful signal, but the signal is *not* in statistical equilibrium with the noise in a telecommunication system.

The main part of this work is organized as follows. In Section 2 we justify the choice of some of the simulation parameters that guarantee that the numerical results are statistically significant (and yet do not require prohibitively long simulation times). The numerical results are reported in Section 3. In Section 4 we summarize our findings. The Appendices contain auxiliary derivations of the mass (a.k.a. number of particles) evolution and a brief description of the numerical method.

2 Estimating required simulation time

The probability of a rogue wave occurrence depends on the magnitude of the nonlinear term in (1) relative to other terms. Therefore, to convincingly show that that probability is affected by noise as opposed to other factors, one must maintain a constant average $|u|^2$. This implies maintaining the ensemble average of the mass

$$N = \int_0^L |u|^2 dx, \tag{4}$$

where L is the length of the considered spatial domain. The evolution equation

$$d\langle N\rangle/dt = 2(D_0 L + C_0\langle N\rangle - \alpha\langle N\rangle) \tag{5}$$

can be derived using the method outlined in Appendix A; here we have ignored the action of the ε-term in (1) for reasons that were explained in the Introduction. Thus, in the statistically steady state,

$$\langle N\rangle_{\mathrm{st}} = D_0 L/(\alpha - C_0). \tag{6}$$

In order to have a specific value of $\langle N \rangle$ in a simulation, one must select values of D_0, C_0, and α satisfying (6). In this work we have always set the parameters so as to maintain the average mass of the solution near the value L:

$$\langle N \rangle \approx L \quad \Rightarrow \quad \frac{1}{L} \int_0^L \langle |u|^2 \rangle \, dx \approx 1. \tag{7}$$

The next issue one needs to address is: In an individual observation (simulation), how much does N fluctuate around its average (6), and what is the time scale of those fluctuations? Answers to these questions will allow us to estimate the simulation time (or the number of simulations with different noise seeds) required to obtain statistics representative of the steady state. Both answers can be obtained from an effective Langevin equation for N, whose approximate form is derived in Appendix A for the case when the noise is purely additive. (When the multiplicative noise is present, the corresponding calculations become more cumbersome and require additional approximations. We do not carry them out because all we need are order-of-magnitude estimates to guide our simulations.) An estimate for the standard deviation of N (for $C_0 = 0$) is

$$\sigma_N = (D_0 L/\alpha) \cdot O(\sqrt{l_{\mathrm{corr},\xi}/L}) = O\big(\langle N \rangle_{\mathrm{st}} \sqrt{l_{\mathrm{corr},\xi}/L} \big), \tag{8a}$$

where $l_{\mathrm{corr},\xi}$ is the correlation length of the noise (defined in Section 3), and the correlation time of N is

$$\tau_{\mathrm{corr},N} = 1/(2\alpha)\,. \tag{8b}$$

The time that it takes the system to reach its steady state is of the same order of magnitude as (8b). An example of evolution of N for a typical set of parameters used in this work is shown in Fig. 1. It confirms the validity of estimates (8).

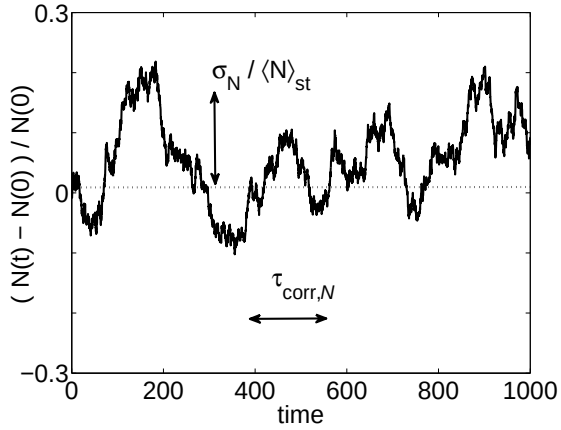

Figure 1: Example of evolution of $N(t)$ for $l_{\mathrm{corr},\xi}/L = 1/36$, $\alpha = 0.0029$, $\beta = 1$, $\gamma = 1$; see Section 3. Double arrows show the estimates (8).

Since $N(t)$ (which is our measure of nonlinearity of the system) fluctuates significantly, it is important to use sufficiently long simulation times, or use a large number of ensemble simulation, to average out the corresponding fluctuations in the probability density function (PDF), $p(|u|)$, of the wave height $|u|$. Such a time can be estimated as follows. In a time interval T there are

approximately $(T/\tau_{\mathrm{corr},N})$ independent "samples" of N, and hence the fluctuations from one such a sample to another get decreased by a factor $\sqrt{T/\tau_{\mathrm{corr},N}}$ when we average over T. Clearly, the count for T should start after the steady state has been reached, i.e. after $t = 1/\alpha$. Also, if one runs n_{simul} ensemble simulations, then the above factor is trivially modified to become $\sqrt{n_{\mathrm{simul}}\, T/\tau_{\mathrm{corr},N}}$.

The estimate in the previous paragraph along with Eqs. (8) shows that the relative size of fluctuations of N, averaged over time T and n_{simul} simulations, scales as

$$\sigma_N/\langle N\rangle_{\mathrm{st}} = O\big(\sqrt{(l_{\mathrm{corr},\xi}/L)/(n_{\mathrm{simul}}\, T\alpha)}\,\big). \tag{9}$$

In all simulations involving noise, reported in the next Section, we set D_0 to a constant value; then (6) and (7) imply that $\alpha = O(D_0)$. Then, we selected parameters so as to ensure

$$\sqrt{(L/l_{\mathrm{corr},\xi})\,(n_{\mathrm{simul}}\, TD_0)} > 50, \tag{10}$$

which according to (9) guarantees that variation of the mass of the solution, averaged over T and all ensemble simulations, are on the order of a few percent. By doubling the length L in selected cases, we verified that condition (10) leads to a similar accuracy of the results reported in the next section. This was sufficient to observe with confidence the effect of increased probability of rogue waves driven by noise, which is the focus of this study. For reference, obtaining the results for entries of most cells reported in Tables 1 and 2 below took between one and two days, using a personal computer running Matlab; the results in Table 2 for $\gamma = 1$ took about three times as long because they required resolution of a wider spectrum.

3 Numerical results and discussion

We considered the following four cases, referring to parameters in (1)–(3).

Case 1 (benchmark): No noise; $D(x) = C(x) \equiv 0$.

Case 2: Additive noise only; $C(x) \equiv 0$.

Case 3: Dominant multiplicative noise; $C_0 = 2D_0L/\langle N\rangle_{\mathrm{st}}$, and since we have always set $N(t = 0) = L$ (see (7)), this amounted to $C_0 = 2D_0$.

Case 4: Dominant additive noise; $C_0 = 0.5D_0L/\langle N\rangle_{\mathrm{st}}$, but only for a subset of parameters of Case 3; see below.

In all Cases we used $\beta = 1$ and considered five values of $\gamma = 0$, 0.1, 0.2, 0.5, 1. This shows how the results scale with the nonlinearity of the system, because we also set the initial conditions to satisfy

$$\frac{1}{L}\int_0^L |u(x,0)|^2 = 1. \tag{11}$$

In Case 1 this guaranteed that $N(t)/L = 1$ during the simulation[2], while in the other Cases we ensured condition (7) by selecting the damping constant (see below). In all cases, the maximum simulated time was $T = 3000$, and we ran simulations with n_{simul} different seeds of noise. (In Case 1 the noise seeds determined the initial condition.) In Cases 2–4, we set $D_0 = 0.003$ and adjusted

[2]Parameter ε was selected so that the relative change of N would be (much) less than 0.1%.

α so as to satisfy (6) with $\langle N\rangle_{\rm st} = 1$; see (7) and (11). In Case 4 we adjusted ε empirically to satisfy the same condition. We also set ε to a value where the high wavenumber damping would be guaranteed to amount for no more than 10% of total dissipation. That value was estimated and adjusted in each case based on the observed width of the solution's Fourier spectrum.

The spectral shapes (3a) of noise in Cases 2–4 were chosen to be Gaussian:

$$G_{\{\xi,\,\eta\}} = \frac{\{D_0,\,C_0\}}{\sqrt{\sqrt{\pi}\;k_{\{\xi,\,\eta\}}}} \exp\left[-\frac{1}{2}\left(\frac{k}{k_{\{\xi,\,\eta\}}}\right)^2\right] \tag{12a}$$

where $k_{\{\xi,\,\eta\}}$ determine the correlation lengths of ξ and η:

$$l_{{\rm corr},\,\{\xi,\,\eta\}} = 2\pi/k_{\{\xi,\,\eta\}}. \tag{12b}$$

In Case 2, for each value of γ we considered two representative values of the noise correlation length, corresponding to $k_\xi = 1$ or 3. In Case 3, for each γ, we considered four combinations of correlation lengths, corresponding to $\{k_\xi,\,k_\eta\} = \{1,\,1\}$, $\{3,\,1\}$, $\{1,\,3\}$, $\{3,\,3\}$. In Case 4, we considered only the combination $\{k_\xi,\,k_\eta\} = \{1,\,1\}$. The purpose of presenting this Case was to demonstrate that even relatively small multiplicative noise may significantly change the solution's PDF. In Case 1, the initial condition had a spectral shape proportional to (12a), and for each γ we also considered two values of its correlation length, $l_{{\rm corr},\,u_0} = 2\pi$ and $2\pi/3$.

To satisfy the statistical accuracy condition (10) with the above values of T and D_0 in Cases 2–4, we used $L = 72\pi$, $n_{\rm simul} = 15$ for $\min\{l_{{\rm corr},\,\xi},\,l_{{\rm corr},\,\eta}\} = 2\pi$ and $L = 36\pi$, $n_{\rm simul} = 10$ for $\min\{l_{{\rm corr},\,\xi},\,l_{{\rm corr},\,\eta}\} = 2\pi/3$. While there is no counterpart of (10) for Case 1, there we also used the same values of L and $n_{\rm simul}$ for the corresponding correlation lengths of the initial condition. We record values of $|u|$ at every grid point and every $t_{\rm rec} = 0.25$ ($t_{\rm rec} \gg \tau_{{\rm corr},\,\xi} \approx 0.02$) starting at $t = 100$ and compute the corresponding PDF $p(|u|)$.

In each cell of Tables 1 and 2 below, we report two numbers: cumulative probability that $|u|$ exceeds 4 average values $|u|_{\rm av} = \int_0^\infty y\,p(y)\,dy$ and excess kurtosis;

$$P_4 = \int_{4|u|_{\rm av}}^{\infty} p(y)dy, \tag{13a}$$

$$\kappa = \frac{\int_0^\infty (y-|u|_{\rm av})^4 p(y)\,dy}{\left(\int_0^\infty (y-|u|_{\rm av})^2 p(y)\,dy\right)^2} - 3. \tag{13b}$$

As a reference, for the Rayleigh-distributed $|u|$, which occurs in the purely linear case with no multiplicative noise, these quantities are:

$$P_4 = 3.5\cdot 10^{-6}, \quad \kappa = 0.25. \tag{13c}$$

Let us note that $|u| \approx 4|u|_{\rm av}$ corresponds to a high, but not extremely high, wave. Indeed, if one assumes that the average *crest* of a wave is approximately twice the average value of $|u|$, then $|u| \approx 4|u|_{\rm av}$ corresponds to a wave whose crest is only about twice as high as the average crest. We chose that moderate value, as opposed to, say, $|u| \approx 6|u|_{\rm av}$, because obtaining significant statistics in the latter case would have taken unrealistically long simulation time when the PDF is close to

Rayleigh. Nevertheless, plots of $p(|u|)$, presented below, show that in the presence of multiplicative noise, the probability of the wave's height exceeding the average *crest* value by 3 or even 4 times, is quite significant. As a reference, we found $|u|_{rmav}$ to be around 0.9 in cases where the PDF has a "lighter" (i.e., Rayleighian-like) tail; it gradually shifted towards smaller values around 0.8 as the tails become heavier.

In Table 1 we show results for Cases 1 and 2; the corresponding PDFs are shown in Figs. 2, 3. These figures show that solutions whose spectra are dominated by low-wavenumber components (as in panels (a)) are considerably more likely to produce rogue waves than those with a greater content of high-wavenumber components. This is consistent with [19], where is was shown that PDFs of spectral components with low wavenumbers (which are different from PDFs reported here) have heavier tails than the Rayleigh distribution. Figure 2 also shows that even for small nonlinearities, the statistics of $|u|$ in the NLS may be non-Rayleighian, depending on the initial condition. A similar result was observed numerically in [20] for different initial conditions than here.

	Case 1		Case 2	
γ	$l_{\mathrm{corr},\,u_0} = 2\pi$	$l_{\mathrm{corr},\,u_0} = 2\pi/3$	$l_{\mathrm{corr},\,\xi} = 2\pi$	$l_{\mathrm{corr},\,\xi} = 2\pi/3$
0	1.5e-6 0.16	1.8e-6 0.20	2.7e-6 0.29	3.2e-6 0.24
0.1	2.7e-4 1.3	3.4e-6 0.28	6.3e-5 2.3	5.3e-6 0.36
0.2	6.1e-4 2.0	5.3e-6 0.33	6.3e-5 2.3	1.6e-5 0.45
0.5	1.8e-3 3.1	2.5e-5 0.59	1.7e-3 3.4	7.7e-5 0.81
1	2.3e-3 3.5	6.9e-5 0.94	2.4e-3 3.7	3.1e-4 1.5

Table 1: In each cell, the numbers listed are P_4 (top) and κ (bottom); see (13). Consistent with statistical accuracy of our simulations, we kept only two significant figures.

Interestingly, these figures also show that the statistics of the pure NLS (Fig. 2), without driving terms, is similar to that of the NLS driven by additive Gaussian noise (Fig. 3). What matters more for statistics is the solution's spectral content rather than the presence of absence of additive random forcing. This observation, however, is substantially altered when one includes multiplicative noise, as we demonstrate below.

In Table 2 we show results for Cases 3 and 4; the PDFs for Case 3 only are shown in Fig. 4. One can see that for higher nonlinearities ($\gamma = 0.5,\ 1$), the multiplicative noise always increases the probability of rogue waves by several orders of magnitude. Even waves whose height exceeds the average *crest* value (see above) by more than a factor of four, occur with a sufficiently high probability of around 10^{-4}.

The most dramatic difference among results shown in different panels of Fig. 4 is seen for

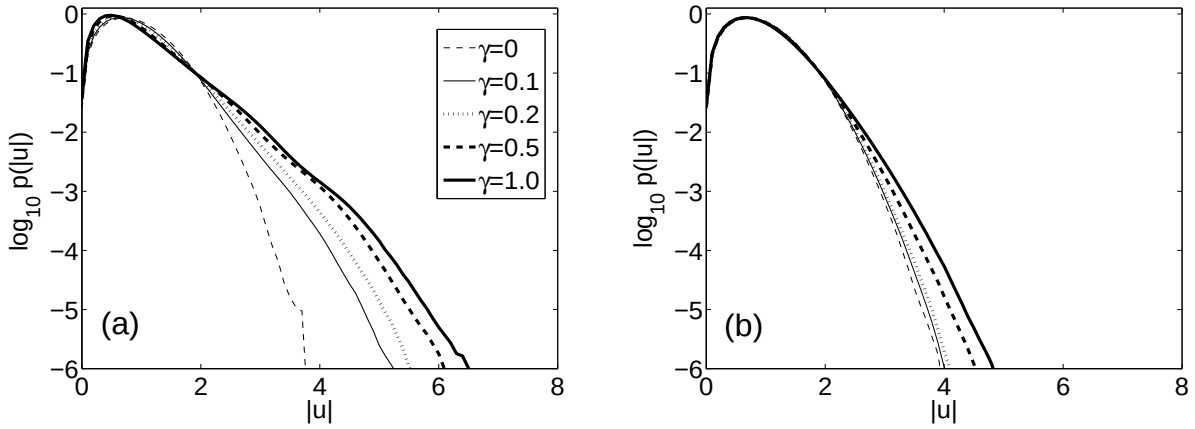

Figure 2: Average PDFs for Case 1. (a): $l_{\mathrm{corr},\,u_0} = 2\pi$; (b): $l_{\mathrm{corr},\,u_0} = 2\pi/3$. In all figures, here and below, the line styles for different values of γ are the same as in panel (a).

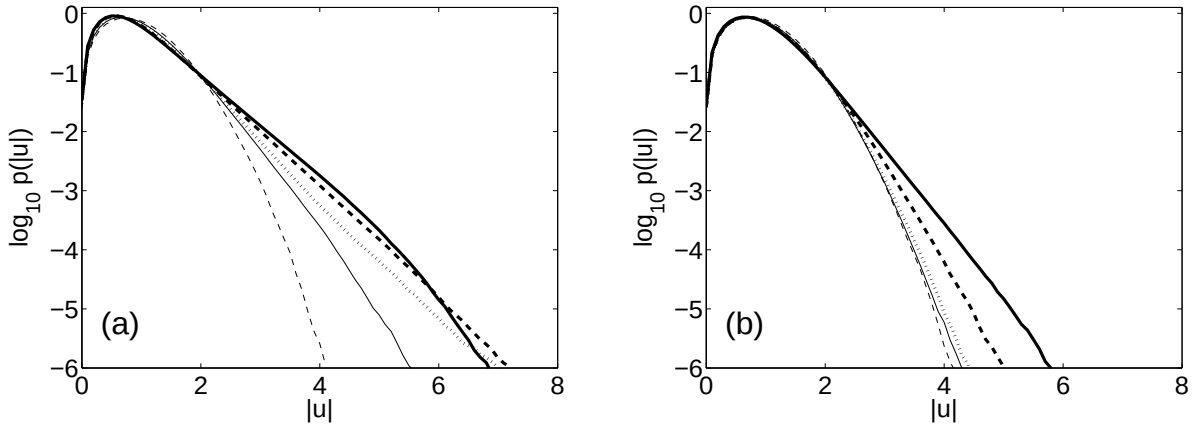

Figure 3: Average PDFs for Case 2. (a): $l_{\mathrm{corr},\,\xi} = 2\pi$; (b): $l_{\mathrm{corr},\,\xi} = 2\pi/3$. Line styles mean the same as in Fig. 2(a).

low nonlinearity, $\gamma = 0.1$. In those cases (see panels (a,c)), multiplicative noise with the larger correlation length leads to a high probability of rogue wave formation, while the correlation length of the additive noise plays a smaller role. Partially, this occurred because in Case 3 the contribution of the multiplicative noise in Eq. (1) is greater than that of additive noise. However, in Case 4, where the relative contributions of additive and multiplicative noises are reversed, one also observes a considerably higher probability of rogue waves that in Table 2 (Case 2) and Fig. 3(a), where only additive noise is present.

4 Conclusions

We have numerically shown that the presence of multiplicative noise with relatively large correlation length increases the probability of rogue waves in the NLS by several orders of magnitude even for low average nonlinearity. Let us point out that this fact cannot be fully explained based on the theory of modulational instability. That theory does indeed predict that for low nonlinearity, it is the low wave numbers, on the order of $\sqrt{(\gamma/\beta)|u|^2}$, that "see" the largest growth (on a plane-wave

	$l_{\mathrm{corr},\xi} = 2\pi$		$l_{\mathrm{corr},\xi} = 2\pi/3$		
γ	$l_{\mathrm{corr},\eta} = 2\pi$	$l_{\mathrm{corr},\eta} = 2\pi/3$	$l_{\mathrm{corr},\eta} = 2\pi$	$l_{\mathrm{corr},\eta} = 2\pi/3$	Case 4
0	8.5e-5	2.3e-5	8.2e-5	1.2e-5	9.0e-6
	0.85	0.55	0.88	0.49	0.41
0.1	3.0e-3	2.9e-4	8.8e-4	2.3e-5	1.4e-3
	13.	2.0	7.2	0.52	6.0
0.2	4.6e-3	7.7e-4	1.9e-3	1.0e-4	3.4e-3
	19.	4.2	12.	0.83	12.
0.5	6.9e-3	2.8e-3	3.8e-3	1.2e-3	5.5e-3
	24.	15.	21.	10.	15.
1	8.5e-3	4.9e-3	4.8e-3	2.7e-3	7.0e-3
	24.	23.	22.	16.	15.

Table 2: Results for Case 3 (first four data columns) and Case 4 (last column); the numbers in each cell mean the same as in Table 1. The parameters $\{l_{\mathrm{corr},\xi},\ l_{\mathrm{corr},\eta}\}$ for Case 4 are the same as those in the first data column.

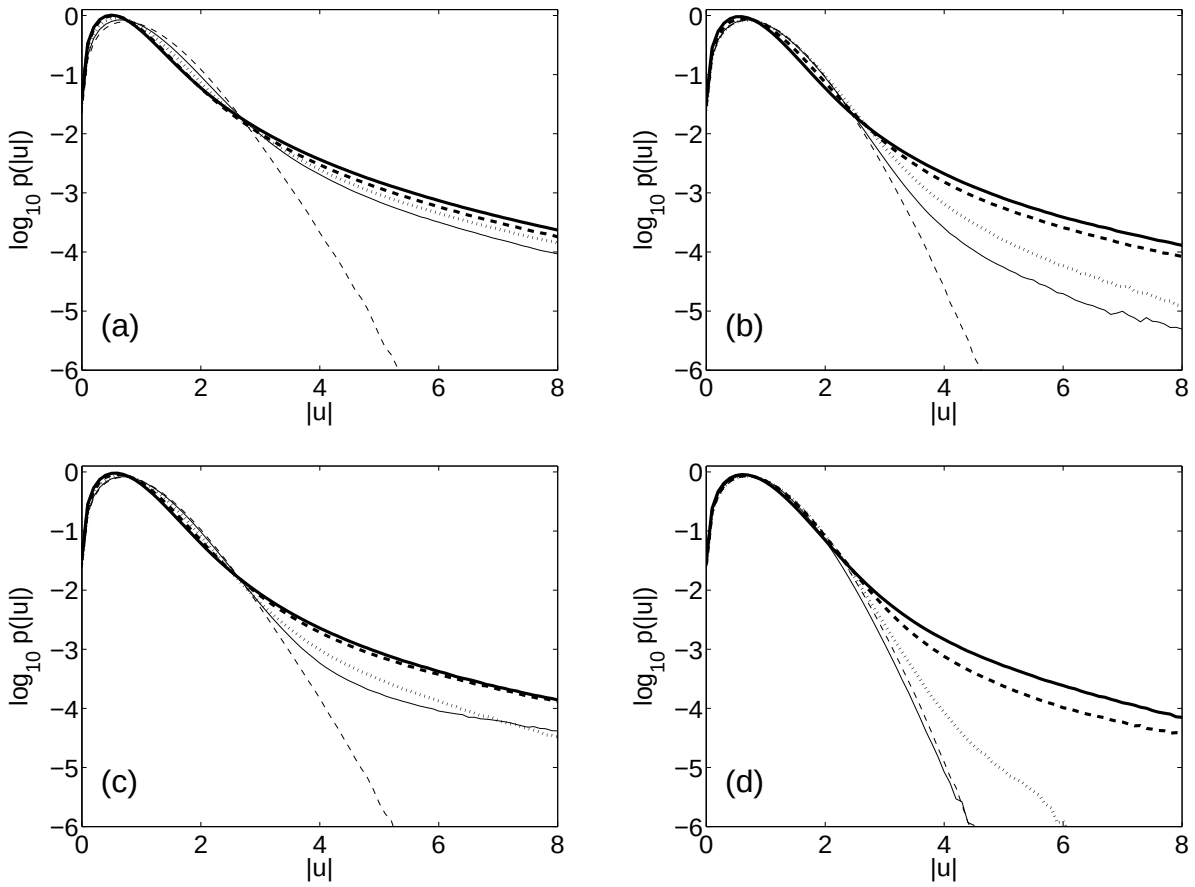

Figure 4: Average PDFs for Case 3 for $\{l_{\mathrm{corr},\xi},\ l_{\mathrm{corr},\eta}\}$ as follows. (a): $\{2\pi,\ 2\pi\}$; (b): $\{2\pi,\ 2\pi/3\}$; (c): $\{2\pi/3,\ 2\pi\}$; (d): $\{2\pi/3,\ 2\pi/3\}$. Line styles mean the same as in Fig. 2(a).

background). However, their growth rate is proportional to $\gamma|u|^2$, i.e. also low. (It is, of course, unclear if the slowly growing perturbations would eventually reach about the same magnitude as

fast growing ones in the nonlinear stage of their evolution.) More importantly, the perturbations' spectral content is not the sole factor determining the evolution: compare the results in Figs. 3(a) and 4(a), where the spectral content of the solution (dominated by low wavenumbers) appears to be similar. It is specifically the multiplicative form of the random forcing that leads to significant probability of rogue wave formation.

The previous observation suggests that further investigation of this phenomenon may include a systematic study of its dependence on the wavelength of the noise, as well as on the relative contributions of the additive and multiplicative forcings. Another direction could be a study of similar phenomena in more realistic models of extreme event formation, which, in particular, would include a more realistic form of high-wavenumber energy dissipation.

Acknowledgement

This work was supported in part by the NSF grant DMS-1217006.

Appendix A: Langevin equation for N

As explained in the main text, the calculations here are done for $\varepsilon = 0$ and $\eta \equiv 0$ in (1). Multiplying that equation by u, subtracting the complex-conjugate expression, and integrating over interval $x \in [0, L]$ using periodic boundary conditions, one finds:

$$dN/dt = -2\alpha N + \nu, \tag{A.1a}$$

$$\nu = i \int_0^L (\xi^* u - \xi u^*) dx. \tag{A.1b}$$

Whenever the arguments (i.e., x and t) of u and ξ are not indicated, they are assumed to be the same. We will handle (A.1a) as a stochastic differential equation for N by approximating ν as

$$\nu = a(N, \ldots) + b(N, \ldots)\chi, \tag{A.2a}$$

where a and b are some functions of N and possibly other functionals of u, and χ is a white noise:

$$\langle \chi(t_1)\chi(t_2) \rangle = \delta(t_1 - t_2). \tag{A.2b}$$

These functions are found below from considering the average and autocorrelation of ν. A similar approach has been used, e.g., in [21].

First, the average of ν over an ensemble of noise realizations is computed using a standard technique (see, e.g., [22]), whereby one represents the solution of (1) as

$$u(t) = u(t - \Delta) + \int_{t-\Delta}^{t} \xi(t_1) dt_1 + O(\Delta). \tag{A.3}$$

Here Δ is a small time interval satisfying

$$\tau_{\mathrm{corr},\xi} \ll \Delta \ll \tau_u, \tag{A.4}$$

where $\tau_{\mathrm{corr},\xi}$ is the correlation time of noise ξ and τ_u is a typical time scale on which u evolves. Then, using (2a), (2c), one has

$$\langle \xi^* u \rangle = D_0, \qquad \langle \xi u \rangle = 0, \tag{A.5}$$

and then from (A.1b) one obtains:

$$\langle \nu \rangle = 2D_0 L. \tag{A.6}$$

Calculation of $\langle \nu(t_1)\nu(t_2)\rangle$ is considerably more complicated, and hence we only indicate its main steps. One needs to compute averages like $\langle \xi^*(x_1,t_1)u(t_1,x_1)\xi^*(x_2,t_2)u(x_2,t_2)\rangle$, which is done using the Isserlis (a.k.a. Wick) theorem for averages of normally distributed variables $g_1,\dots,g_4$:

$$\langle g_1 g_2 g_3 g_4 \rangle = \langle g_1 g_2 \rangle \langle g_3 g_4 \rangle + \langle g_1 g_3 \rangle \langle g_2 g_4 \rangle + \langle g_1 g_4 \rangle \langle g_2 g_3 \rangle \,, \tag{A.7}$$

Eqs. (A.5), and the fact that terms like

$$\langle \xi^*(x_1,t_1)u(x_2,t_2)\rangle \langle \xi^*(x_2,t_2)u(x_1,t_1)\rangle = 0 \tag{A.8}$$

due to $\tau_{\mathrm{corr},\,\xi} \ll \tau_u$. The result is:

$$\langle \nu(t_1)\nu(t_2)\rangle = (2D_0L)^2 + \langle W(t_1)\rangle \delta(t_1 - t_2), \tag{A.9a}$$

where

$$W(t) = 2\int_0^L \int_0^L D(x_1 - x_2)(u^*(x_1,t)u(x_2,t) + u(x_1,t)u^*(x_2,t))\, dx_1 dx_2. \tag{A.9b}$$

(Note that if $D(x_1 - x_2) \propto \delta(x_1 - x_2)$, then $W \propto N$, as in [21].) Thus, one needs an evolution equation for W. However, for our *estimation* of the dynamics of N, we have used the stationary average value $\langle W \rangle_{\mathrm{st}}$. It is found similarly to the above, where one also needs an average $\langle (|u_1|^2 - |u_2|^2) u_1 u_2^* \rangle$; we have denoted $u_{1,2} \equiv u(x_{1,2},t)$. It can be *approximated* by zero using (A.7), as is standard in the application of the Wigner function formalism to random NLS-like models (see, e.g., [23]). As a result,

$$d\langle W \rangle / dt = -2\alpha \langle W \rangle + 8 \int_0^L \int_0^L (D(x_1 - x_2))^2 \, dx_1 dx_2, \tag{A.10}$$

whence

$$\langle W \rangle_{\mathrm{st}} = (4/\alpha) \int_0^L \int_0^L (D(x_1 - x_2))^2 \, dx_1 dx_2 \equiv (8\pi L/\alpha) \int |G_\xi(k)|^4 dk, \tag{A.11}$$

where we have also used (3b).

To satisfy (A.6) and (A.9a), it suffices to set $a = 2D_0L$ and $b = \sqrt{\langle W \rangle_{\mathrm{st}}}$ in (A.2), so that (A.1a) becomes:

$$dN/dt = -2\alpha N + 2D_0 L + \sqrt{\langle W \rangle_{\mathrm{st}}}\, \chi. \tag{A.12}$$

This is an Ornstein–Uhlenbeck process with a nonzero mean. Its standard deviation and correlation time are given by

$$\sigma_N = \sqrt{\langle W \rangle_{\mathrm{st}} / (4\alpha)}, \tag{A.13}$$

and Eq. (8b), respectively (see, e.g., Sec. 2.4 in [15]). The time required for the PDF of N to approach its stationary form can be found from the eigenvalue analysis of the Fokker–Planck equation corresponding to Eq. (A.12). However, it can also be directly estimated from (A.12) itself to be $O(1/\alpha)$, which is the same as (8b).

The order-of-magnitude estimate (8a) is found from (A.13), (A.11) as follows. As in Section 3, we assume the Gaussian spectrum (12) for the noise. Then

$$\sigma_N = (D_0 L/\alpha)\sqrt{4\sqrt{2\pi}\,/(k_\xi\, L)}, \tag{A.14}$$

which with $l_{\mathrm{corr},\,\xi} = 2\pi/k_\xi$ yields (8a).

Appendix B: Numerical method for (1)

One of the key requirements for the numerical method is that it should correctly reproduce averages (A.5), on which we base our consideration of a statistically constant $\langle N\rangle$. Since these averages are founded in the Stratonovich interpretation of the noise, all we need is to model noise as having small but finite correlation time. Fortunately, this does not require us to reduce the simulation time step because it is forced to be small by a separate requirement of *stability* (rather than accuracy) of the numerical method; see below.

Thus, we model the noise terms as an Ornstein–Uhlenbeck process. In continuous time, it is:

$$\xi_t(x,t) = \left(-\xi(x,t) + \int G_\xi(k)\hat{w}(k,t)e^{-ikx}dk\right)/\tau_{\mathrm{corr},\,\xi}\,, \tag{B.1}$$

and similarly for η; see (A.4) and (3a) for notations. One can show that it satisfies (2). In discrete time $t_n = n\Delta t$, we approximate (B.1) by the first-order Euler method:

$$\xi_{n+1} = (1 - \Delta t/\tau_{\mathrm{corr},\,\xi})\xi_n + \sqrt{\Delta t}/\tau_{\mathrm{corr},\,\xi}\int G_\xi(k)\hat{w}_n(k)e^{-ikx}dk, \tag{B.2}$$

where $\hat{w}_n$ are independent, complex-valued random variables with unit variance of their real and imaginary parts, and the integral over k is, in fact, a discrete sum. We will comment on the accuracy of this simple approximation later. While we used different spectral functions, $G_\xi(k)$ and $G_\eta(k)$, for the additive and multiplicative noises, we used the same correlation time, $\tau_{\mathrm{corr},\,\xi}$, for both of them.

We have experimented with several ratios of $\Delta t/\tau_{\mathrm{corr},\,\xi}$ and found that as long as one has

$$\Delta t \ll \tau_{\mathrm{corr},\,\xi} \ll \tau_u = O(1), \tag{B.3}$$

the results are not sensitive to the exact value of $\Delta t/\tau_{\mathrm{corr},\,\xi}$. Let us also stress that due to this ratio being small, ξ and η can be treated as regular, i.e., *continuous*, functions of time, thus obviating the need to employ any special methods for stochastic systems. In all simulations we used $\tau_{\mathrm{corr},\,\xi} = 0.018$, so that $\Delta t/\tau_{\mathrm{corr},\,\xi}$ was either $1/45$ (for $\gamma = 1$) or $1/20$ (for $\gamma < 1$); see below.

To solve (1) with the already determined ξ and η, we used the first-order split-step method:

$$u_{n+1} = \mathcal{F}^{-1}\left[e^{-(i\beta k^2+\varepsilon k^4)\Delta t}\,\mathcal{F}\left[e^{i\gamma|u_n|^2\Delta t}u_n\right]\right]\, e^{-i(\alpha+i\eta_{n+1})\Delta t} \;-\; i\xi_{n+1}\Delta t\,, \tag{B.4}$$

where $\mathcal{F}$ and $\mathcal{F}^{-1}$ are the Fourier transform and its inverse. In addition to the common two stages — nonlinearity and dispersion, — this method also has a linear multiplicative (with α and η) and additive (with ξ) stages. In principle, these two stages could be combined into one, which would make the form of the last term in (B.3) more complicated. We have conducted tests with that other form and did not observe any noticeable differences in solution $u(x,t)$ (using the same seeds of noise for both methods). We have also compared out simple method with the exact solution of (1) which can be found when $\gamma = 0$ and η does not depend on x; in that case, also, the numerical and exact solution were within $O(\Delta t)$ of each other, as expected. Finally, we have also employed the implicit trapezoidal method instead of (B.2) for solving (B.1), and, again, differences were imperceptible.

We now comment on the time step Δt. By the stability condition of the split-step method (with $\alpha = 0$ and no noise terms), one needs to have [24, 25]:

$$\Delta t < \pi / k_{\max}^2. \tag{B.5}$$

In all simulations with $\gamma < 1$, we used $k_{\max} = 2^9/9 \approx 57$ and hence selected $\Delta t = 0.0009$. For $\gamma = 1$, we used a 50% wider spectrum (by reducing L); accordingly, we then used $\Delta t = 0.0004$.

References

[1] N. Akhmediev, J.M. Dudley, D.R. Solli, S.K. Turitsyn, J. Opt. 15 (2013) 060201.

[2] P.T.S. DeVore, D.R. Solli, D. Borlaug, C. Ropers, B. Jalali, J. Opt. 15 (2013) 064001.

[3] K. Dysthe, H.E. Krogstad, P. Müller, Annu. Rev. Fluid Mech. 40 (2008) 287.

[4] M. Onorato, S. Residori, U. Bortolozzo, A. Montinad, F.T. Arecchi, Phys. Rep. 528 (2013) 47.

[5] D.R. Solli, C. Ropers, P. Koonath, B. Jalali, Nature 450 (2007) 1054.

[6] K.B. Dysthe, Proc. Roy. Soc. A 369 (1979) 105.

[7] F. Fedele, Z. Cherneva, M.A. Tayfun, C. Guedes Soares, Phys. Fluids 22 (2010) 036601.

[8] A.I. Dyachenko, V.I. Zakharov, JETP Lett. 93 (2011) 701.

[9] A. Pushkarev, V.E. Zakharov, Physica D 248 (2013) 55.

[10] F. Fedele, J. Fluid Mech. 748 (2014) 692.

[11] A. Hasegawa, Y. Kodama, Solitons in Optical Communications, Clarendon Press, Oxford, 1995; Sec. 5.3.

[12] T.I. Lakoba, J. Lightwave Technol. 22 (2004) 382.

[13] D. Cai, A.J. Majda, D.W. McLaughlin, E.G. Tabak, Physica D 152–153 (2001) 551.

[14] V.E. Zakharov, F. Dias, A. Pushkarev, Phys. Rep. 398 (2004) 1.

[15] W. Horsthemke, R. Lefever, Noise-Induced Transitions: Theory and Applications in Physics, Chemistry, and Biology, Springer, Berlin, 1984.

[16] S. Leblanc, Phys. Fluids 19 (2007) 101705.

[17] S.Y. Annenkov, V.I. Shrira, Phys. Rev. Lett. 107 (2011) 114502.

[18] A. Slunyaev, A. Sergeeva, E. Pelinovsky, arXiv preprint 1407.2443 (2014).

[19] Y. Choi, Y.V. Lvov, S. Nazarenko, B. Pokorni, Phys. Lett. A 339 (2005) 361.

[20] D.S. Agafontsev, V.E. Zakharov, arXiv preprint 1202.5763v4 (2012).

[21] C.J. Mckinstrie, T.I. Lakoba, Opt. Express 29 (2003) 3628.

[22] W.T. Coffrey, Yu.P. Kalmykov, J.T. Waldron, The Langevin Equation, World Scientific, Singapore, 2004; Sec. 1.10.

[23] I.E. Alber, Proc. Roy. Soc. Lond. A 363 (1978) 525.

[24] J.A.C. Weideman, B.M. Herbst, SIAM J. Numer. Anal. 23 (1986) 485.

[25] T.I. Lakoba, J. Opt. Soc. Am. B 30 (2013) 3260.